Graphical Abstract (for review)

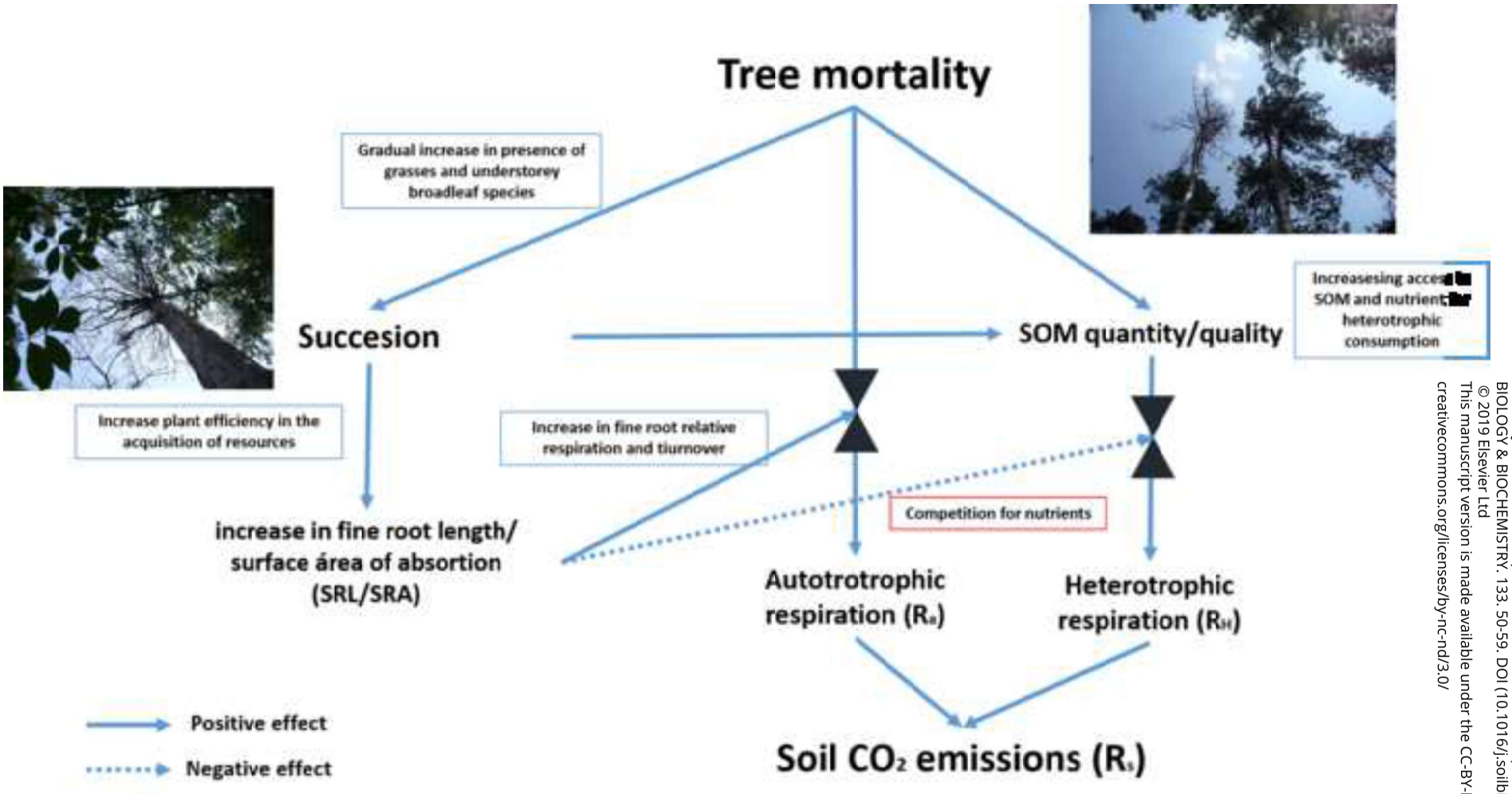

***Highlights (for review)**

Highlights

- Episodes of drought-induced conifer mortality are becoming more frequent in Europe
- Conifer mortality triggers secondary succession of autochthonous broadleaf species.
- Tree mortality triggers complex cascading effects which ultimately affects R_s
- Changes in fine root specific root length (SRL) correlates negatively with R_H.

Cascading effects associated with climate-change-induced conifer mortality in mountain temperate forests result in hot-spots of soil CO_2 emissions

Curiel Yuste J. [1,2*], Flores-Rentería D.[3], García-Angulo D.[4], Hereş A.-M.[1,5], Bragă C.[6], Petritan A.-M.[6], Petritan I.C.[5]

[1] BC3 - Basque Centre for Climate Change, Scientific Campus of the University of the Basque Country, 48940 Leioa, Spain;
[2] IKERBASQUE - Basque Foundation for Science, Maria Diaz de Haro 3, 6 solairua, 48013 Bilbao, Bizkaia, Spain
[3] CONACYT- CINVESTAV Unidad Saltillo, Group of Sustainability of Natural Resources and Energy. Av. Industria Metalúrgica 1062, Parque Industrial Ramos Arizpe, Ramos Arizpe, 25900, Coahuila, Mexico.
[4] Museo Nacional de Ciencias Naturales (MNCN, CSIC) Serrano 115 dpdo; E-28006 Madrid, Spain.
[5] Department of Forest Sciences, Transilvania University of Braşov, Şirul Beethoven -1, 500123 Braşov, Romania
[6] National Institute for Research-Development in Forestry 'Marin Dracea', Bulevardul Eroilor, Voluntari, 077190, Romania

*Corresponding author: Tlf: +34 944014690; e-mail= jorge.curiel@bc3research.org

Keywords: *Soil respiration, heterotrophic respiration, secondary succession, tree mortality, fine roots functional traits, cascading effects*

Summary

As a widespread phenomenon affecting terrestrial ecosystems worldwide, the extent and spatio-temporal scales at which the increasing number of reported events of climate-change-induced tree mortality could affect the ecology and carbon (C) sink capacity of terrestrial soils, remains unknown. We here study how regional-scale drought-induced tree mortality events registered after a very dry 2012 year in the Carpathians mountain range (Romania), which affected three of the most widely distributed conifer species: Scots pine, Black pine, and Silver fir, resulted in hot-spots of biogenic soil CO_2 emissions (soil respiration; R_s). Four to five years after the main mortality event, R_s-related soil CO_2 emissions under dead trees were, on average, 21% higher than CO_2 emissions under living trees (ranging from 18 to 35%). Total (R_s) and heterotrophic (R_H)-related soil CO_2 emissions were strongly determined by the soil environmental alterations following tree mortality (e.g. changes in quantity and quality of soil organic matter, microclimate, pH or fine root demography). Moreover, the massive mortality event of 2012 ultimately resulted in a stronger dominant role of successional vegetation (broadleaf seedlings, shrubland and grasses) in controlling those environmental factors that either directly or indirectly affected biotic soil fluxes (R_s and R_H). We, therefore, show that apart from the well-known direct effects of climate change over soil CO_2 emissions, cascading effects triggered by climate-change-induced tree mortality could also exert a strong indirect impact over soil CO_2 emissions, altering the magnitude and the environmental controls of R_s and hence determining ecosystem C budget and their response to climate.

1. Introduction

The number of episodes of forest defoliation and mortality associated with climate change has increased substantially during the last decades (Allen et al., 2010; Carnicer et al., 2011), and it is further expected to increase even more in future decades (IPCC 2014). In this regard, understanding physiological and ecological causes of tree mortality as well as predisposition of trees to die is nowadays a hot-topic that has attracted many attention and studies (Allen et al., 2010, 2015; Anderegg et al., 2012; McDowell et al., 2015; Sangüesa-Barreda et al. 2015; Rogers Brendan et al., 2016; Neumann et al., 2017; Lloret and Kitzberger, 2018). There is, however, a knowledge gap on how ecosystems are actually responding to such perturbations, i.e. whether and at which extent tree mortality could affect ecosystem functioning (Anderegg, et al. 2013) and more particularly how tree mortality could affect soil respiration (R_s), which represents the total biogenic CO_2 produced and emitted from soils (Vargas et al., 2010), and is the major outgoing flux of CO_2 from ecosystems to the atmosphere (Curiel Yuste et al., 2005; Davidson et al., 2005; Barba et al., 2018). Trees have the capacity to modulate the belowground environment (Flores-Rentería et al., 2015, 2016) triggering cascading causal-effect relations that could result in substantial changes in the biological functioning of the soil system and in fundamental alterations of the soil nutrient and soil CO_2 emissions (Flores-Rentería et al., 2018). However, data and evidences on how these alterations occur and at which extent tree mortality could affect patterns and controls of CO_2 emissions from terrestrial soils are scarce.

Besides altering soil abiotic conditions, tree mortality limits the supply of substrate in the form of carbohydrates (e.g. exudates) or nutrients (litter) demanded by belowground organs

70 (fine roots), symbionts (e.g. mycorrhiza), and soil biological communities from the
71 rhizosphere and the soil (e.g. Högberg et al., 2001; Binkley et al., 2006; Barba et al., 2016).
72 The disruption of the C flow to belowground has been directly related to almost immediate
73 decreases in R_s (Högberg et al., 2001; Binkley et al., 2006; Nave et al., 2011; Levy-Varon
74 et al., 2014), due to a parallel decrease in autotrophic (fine root and mycorrhiza) and
75 heterotrophic (respirations from microbes and soil fauna) respiration. On medium-long
76 term, the death of trees may have critical effects over key soil biogeochemical cycling
77 (Rodriguez et al. 2016), resulting in chronical losses of key nutrients such as nitrogen (N),
78 with unknown consequences for the capacity of the systems to recover pre-perturbations
79 pools and functions (García-Angulo et al. in prep). This happens because the disruption of
80 the flow of C from plants to soils and the changes in the microclimatic conditions
81 associated with tree mortality may prominently alter the composition, structure and
82 functionality of soil biological communities (Curiel Yuste et al. 2012, Avila et al. 2016)
83 resulting in irreversible losses of key functional groups that sustain important soil functions
84 such as N fixation or mineralization of essential nutrients (Gómez-Aparicio et al. 2017).
85
86 Few studies have been designed, however, to investigate in depth how processes triggered
87 by tree mortality could affect biogenic soil CO_2 emissions and at which extent. In this
88 regard, tree mortality has been associated with ecosystems reaching new equilibriums,
89 resulting in important changes in the diversity of soil biota and soil functions (Curiel Yuste
90 et al., 2012; Lloret et al., 2015, Avila et al., 2016), as well as in the overall biogenic
91 emissions of CO_2 from soils (Moore et al. 2013; Avila 2018). Depending on the magnitude
92 of the tree mortality event and/or legacies from historical management, forest ecosystems
93 are able to counteract potential negative effects of tree mortality and recover pre-

94 perturbations functioning rates relatively fast (Nave et al., 2011; Gough et al., 2013; Levy-
95 Varon et al., 2014; Barba et al., 2016). This is because tree mortality, depending on the
96 ecosystem's characteristics and its initial conditions, triggers a process of recolonization by
97 seedlings of the same species (regeneration) or of other species better fitted to present
98 conditions (secondary succession), which slowly replace the niche left by the death of the
99 trees (e.g. Vayreda et al., 2016; Ruiz-Benito et al., 2017). How these complex aboveground
100 ecological processes could actually impact belowground functioning, subsequently
101 affecting magnitude and controls of biotic CO_2 emissions remains unknown.
102
103 The objective of this study was to deepen our mechanistic understanding of the effects of
104 large-scale tree die-off events on total soil respiration (R_s). For that, we here show a
105 regional scale study, spanning for two consecutive years (2016, "year 1"; and 2017, "year
106 2"), on rates of R_s in stands located in the Carpathians mountain range (Braşov county,
107 Romania), where recent extremely dry years, such as 2012, have resulted in extended
108 mortality rates. These mortality events have mainly affected conifer tree species, especially
109 Scots pine (*Pinus sylvestris* L.), Silver fir (*Abies alba* Mill.), and Black pine (*Pinus nigra*
110 Arnold*)*. The conifers' mortality observed in 2012 and estimated to extend over large areas
111 in the forests situated at different altitudes around Braşov (Forest Districts of Râşnov,
112 Săcele, and Kronstadt), followed a sequence of several extraordinary dry and hot years
113 registered during the first decade of the century
114 (http://www.meteoromania.ro/anm/?lang=ro_ro). These affected conifers are slowly
115 replaced by autochthonous broadleaf species, especially *Quercus robur*, *Fagus sylvatica,*
116 *Fraxinus ornus, Fraxinus excelsior, Carpinus betulus, Quercus petraea or Acer campestre*
117 *(Table 1)*. Additionally, the study collected detailed information on variables potentially

118 sensitive to tree die-off and directly/indirectly associated with R_s, e,g, soil water content
119 (SWC) and temperature (Tsoil), soil C and nutrients pools, soil heterotrophic respiration
120 (R_H), and fine root biomass and functional traits (e.g. specific root area, SRA and root
121 length, SRL).
122
123 We, therefore, hypothesized that abiotic/biotic changes promoted by tree mortality will
124 trigger a cascade of causal-effect relations that could have resulted in substantial changes in
125 the biological functioning of the soil system, subsequently altering the soil CO_2 emissions.
126 In particular, we hypothesized that in these coniferous forests, where tree mortality is
127 giving way to forests dominated by native hardwood species, the process of secondary
128 succession associated with mortality of conifers would be associated with profound
129 transformations of the microclimate, biology and chemistry of the soil, which ultimately
130 will affect the magnitude and controls of soil CO_2 emissions.
131
132 **2. Materials and Methods**
133 *2.1. Study sites*
134 For this study, we selected a total number of 9 conifer stands (3 for Silver fir, 3 for Scots
135 pine, and 3 for Black pine), all of them affected by recent mortality events (i.e., following
136 the 2012 drought) (Table 1). These forests were located in the Transylvanian side of the
137 Eastern Romanian Carpathians Mountain range (Braşov County). As we wanted to
138 avoid/limit as much as possible other disturbance factors (e.g. management), forests were
139 selected either in protected areas or in areas where management intensity has been minimal
140 for the last decades. All stands were located on sloppy terrains (slopes ranging from 17 at to
141 37 º). Both pine species stands were located between ≈ 450 and 700 m a.s.l., while the

142 Silver fir stands were situated starting from ≈ 800 m a.s.l) (Table 1). Both pine species are
143 almost pure stands, that were artificially regenerated ≈100 years ago, whereas the Silver fir
144 stands are uneven, naturally regenerated, mixed stands with *Fagus sylvatica* (up to 35% in
145 the forest composition) of more than 150 years old (Hereş et al., in prep). Soil type in the
146 Silver fir stands is mainly Eutricambisols, while Rendzina is the main soil type of the pine
147 stands (Table 1). Both mean annual precipitations (MAP) and mean annual temperatures
148 (MAT) (Climate Research Unit Time Series, CRU TS3.10; via http://climexp.knmi.nl)
149 were relatively low and not very variable among locations, ranging, respectively from 593
150 to 693 mm and from 3.7 to 6.6 ºC (Table 1). Our study also shows a natural understory
151 gradient (tree saplings and seedlings) and grass cover, from sites with very scarce
152 understory/grass cover (7%) to sites with understory/grass cover averaging up to 70%
153 (Table 1). The drought-induced mortality rate was estimated to round 19-23% for Silver
154 fir, 16-27% for Black pine, and 17-22% for Scots pine (Table 1).
155
156 *2.2.Field measurements*
157 *2.2.1. Experimental design and tree age estimation*
158 At each of the 9 conifer stands affected by mortality, 5 pairs of standing adult dead and
159 living trees were sampled (see below) along a transect perpendicular to the slope. We used
160 a paired sampling design (Bigler and Bugmann 2004), in which the selected living trees had
161 similar size (diameter at breast height, DBH), competition level, and microsite conditions
162 with the dead ones. Trees noticeably affected by biological agents (e.g. pathogens, fungus),
163 wind, or human influences were avoided during the sampling. The sampling of the 5 pairs
164 was carried out in transects starting at a random point within each stand and maintaining a
165 constant altitude, and thus similar humidity conditions, until the required number of trees

were sampled. Distance between sampled pairs was always >5 m. To establish the age of the living trees and the mortality year for the dead trees, from each tree, two wood cores were extracted at breast height (1.3 m), approximately orthogonal to the slope, using increment borers (Hereş et al., in prep). At the same time, for all trees, we recorded the following variables: species, status (dead or living), DBH, height and crown diameters. All trees within a 5 m radius from the trunk of the sampled trees (i.e., reference trees) and with a DBH>10 cm were inventoried, and their taxonomic identity (species), DBH and distance to the reference sampled trees were registered. We calculated a tree competition index as the sum of the diameters of all trees with DBH>10 cm within 5 m radius around the reference tree. Within the same considered 5 m radius, the percentage cover (%) of the understory vegetation (woody species with a DBH < 10 cm, shrubs) and grass cover were visually assessed. To quantify light availability, we took a hemispherical photo near every collar during the 2016 summer with a Nikon digital camera with fisheye lens and a self-leveling mount. Photos were processed with the Winscanopy software (Regents Instruments Inc., Sainte-Foy, Quebec, 2003). As a measure of light intensity, we used the total site factor (TSF) in percent of above canopy light, and LAI (leaf area index).

2.2.2. Soil respiration (R_s) measurements

Starting from spring 2016 ("year 1"), at each study site two PVC collars (10 cm in diameter, and 8 cm in height) per each of the selected dead and living trees were inserted into the soil at an average depth of 2.5 cm to measure R_s. Collars set at this depth were stable and caused minimal disturbance to fine roots. They were installed at around a 50 cm distance, on the left and right-hand sides of the trunk of each sampled living and dead tree, in a fictitious line perpendicular to the slope. Measurements of R_s were carried out within

each collar with a portable infrared gas analyzer (IRGA) connected to a soil respiration chamber (EGM-4 and SRC-1; PP Systems, USA). We further added the to the chamber volume of the commercial chamber (1171 cm^3) the extra volume generated from the collars. The increase of CO_2 within the chamber was measured during 120 seconds. Soil CO_2 efflux measurements were always performed between 9 a.m. and 6 p.m. R_s was not measured during rainy days. When a major rain event occurred (e.g., daily precipitation > 15 mm), R_s measurements were postponed 36 h in order to minimize the effects of extreme precipitation on R_s. Each R_s measurement campaign was performed within an interval of 3-4 days. In total, R_s measurements were performed in 7 different time series: April 2016 (spring), July 2016 (summer), September 2016 (autumn), November 2016 (winter), April 2017 (spring), July 2017 (summer), and October 2017 (autumn), covering thus all seasons. Periods when the snow layer was thick, covering the soil, were not considered.

Both soil temperature (Tsoil) and soil water content (SWC) were measured simultaneously with R_s. Tsoil was measured using a Soil Temperature Probe (STP, PP Systems) that was inserted at 5 cm depth into the soil. Soil water content (SWC) was measured at 6 cm depth, using the ThetaProbe ML2X soil moisture sensor (Delta-T Devices, UK) coupled to a data logger (Infield7, UMS GmBh Munchen). We performed 3 different measurements of soil moisture around each collar and recorded the average value of them which was used in further analyses.

2.2.3. Soil sampling

Apart from the R_s measurement campaigns, a campaign was carried out for the collection of soil samples in late summer 2016 (first week of August). We collected soil samples near

each PVC collar to determine: soil chemical composition, R_H, fine root biomass, and the different fine roots functional traits (see below). We sampled three soil cores in about maximum 10 cm distance around each PVC collar. Soil cores were taken using a cylinder tube sampler (diameter of 5 cm) that was introduced at a depth of 10 cm in the soil after removing the not yet decomposed litter (O_L horizon) of the previous year. Afterwards, all three soil cores were merged into one single composite sample per each PVC collar, put into bags and stored at cool temperature (<4^{o}C) in mobile ice boxes till further processing in the lab. A total of 180 composite soil samples (9 conifer sites x 5 tree couples x 2 status (living and dead) x 2 PVC collars per each sampled tree) were collected.

2.3.Laboratory analyses

2.3.1. Chemical and physical soil analysis

In the laboratory, soil water content (SWC) for each soil sample collected in 2016 was measured gravimetrically by sampling 20 g of fresh soil (avoiding stones), and drying it at 105^{o}C during 48 hours. Both stones and roots (fine and coarse) were manually separated from all collected soil samples. Stones were then weighted to obtain their total mass. The remaining soil was sieved at 2 mm, dried and stored in a dark place for subsequent analyses. Water Holding Capacity (WHC) and bulk density (McKenzie et al, 2014) were calculated, and soil pH was measured in distilled water with a soil – H_2O ratio of 1:20 for each soil sample.

To analyze the concentrations of total organic carbon (TOC), and nitrogen (TN) and nutrient content in soils, the sieved soil was further grinded by hand using a mortar and then divided in two aliquots. One aliquot was used to calculate the nutrient content (Al,

Mg, K, Na, P, Ca, S, and Mn) of the soil using an inductively coupled plasma optical emission spectrometry (ICP-AES; Thermo Scientific iCAP 6500DUO, ThermoFisher Scientific, Waltham, MA, USA), while the other aliquot was used to measure the TOC and TN using an elemental analyzer (TruSpec CN, LECO, Saint Joseph, MI, USA).

2.3.2. Root measurements

All the roots that were separated from each soil sample (see above) were first carefully cleaned with distilled water to remove adhered soil particles and then sorted into two diameter classes: fine roots (diameter < 2 mm) and coarse roots (diameter > 2mm). No distinctions between fine roots from grasses and trees could be made. Cleaned fine roots were then scanned and processed with WinRHIZO (Regents Instruments Inc., Quebec, Canada) to obtain fine root length, fine root diameter, and fine root surface area. Finally, both fine and coarse roots were dried at 65^{o}C for 5 days to reach a constant weight, and afterwards weighed to the nearest 0.1 g. Based on these measures we determined the demography of the fine root population based on different fine root functional traits: fine root biomass (FRB, g/g soil), fine root volume (FRV, cm3/g soil), specific root length (SRL, ratio of fine root length to dry weight, m g^{-1}) and specific root area (SRA, ratio of fine root area to dry weight, cm^2 g^{-1}).

2.3.3. Soil R_H measurements under controlled conditions

R_H was measured using 40 g of dry, sieved soil that was introduced into a sample jar of 150 mL volume and was rewetted to 60 % of its WHC. Once the desired WHC was achieved, this soil was incubated 48 hours in an environmental chamber (at 20 º C and 80% of moisture) to avoid potential anomalous pulses of CO_2 (“Birch effect”; Birch, 1958).

Afterwards, it was again incubated controlling water content, this time following a temperature gradient from 5 to 35 º C to cover a wide range of temperatures. R_H was measured every 10 º C (i.e., 5 ºC, 15 ºC, 25 ºC, and 35 ºC) during 60 seconds with an EGM-4 and the net CO_2 increases were calculated following a similar protocol to that of Curiel Yuste et al. (2007, 2011). The R_H that we further used to do analyses represents the averaged of the R_H values measured at each temperature (i.e., 5 ºC, 15 ºC, 25 ºC, and 35 ºC), thus covering the R_H variability of this microclimatic range.

2.4.Statistical analysis

A principal component analysis (PCA) was conducted to reduce the n-dimensional of soil nutrients data into two linear axes explaining the maximum amount of variance (Supplementary material, Fig. S1). According to the plot of the two first PCA components the soils' elemental composition splits as it follows: PC1 reflects a gradient of nutrients' availability related with higher amounts of C, N, P, Ca, S, and Mg, whereas PC2 reflects a gradient of soil organic matter (SOM) availability (Fig. S1). Hence, both PC1 and PC2 were subsequently used in models as a measure of the nutritional status and of the substrate available in soils.

We performed a preliminary evaluation of the potential effects of inter-annual variability (year 1 vs year 2), tree species (Silver fir, Scots pine, and Black pine), and tree status (differences among dead and living trees) over R_s and soil microclimate (Tsoil and SWC). To do so, we firstly averaged R_s, Tsoil and SWC values for the two different PVC collars installed per each tree (see above *Soil respiration (R_s) measurements*) at each field campaign. Since none of the variables were normally distributed, we used a non-parametric

one-way analyses of variance (Kruskal-Wallis tests) followed by a pairwise Wilcoxon post-hoc test with a Bonferroni correction.

Because our first aim was to investigate the drivers of soil CO_2 production across this regional gradient we used linear mixed-effects models (nlme R package; Pinheiro et al., 2016) to analyze the influence of tree mortality and environmental data (e.g. biotic and abiotic variables that could potentially affect R_s) on R_s and R_H. In order to focus in drivers of R_s and R_H variability across sites we then averaged all seasonal values (n=7) to one single averaged value per tree. As R_s and R_H data were not normally distributed, we logarithmic transformed them. The model was "forced" to include tree status as a fixed variable in order to test and further discuss potential differences in fluxes and controls associated to tree status. Besides the status of the tree, the fixed part of the models also accounted for other environmental factors that could explain variability in R_s and R_H: e.g. soil microclimatic conditions (Tsoil and SWC), aboveground tree and forest structure (DBH, Tree competition index or yunderstorey/grass cover), SOM content (PC2), soil nutritional status (PC1), fine root biomass (FRB), and fine root specific length/area (SRL/SRA). For all models tree species nested within site identification were introduced as a random effect. To look for differences between vigor groups, the least-squares means were analyzed applying a Tukey correction. The coefficients were estimated using the restricted maximum likelihood method. The residuals of the models fulfilled the conditions of normality ($p > 0.05$). The selection of the final models was based on the Akaike's information criterion (AIC) (i.e. minimal models with the lowest AIC).

309 Structural equation models (SEMs) were finally used to test the direct and indirect
310 influence of the different biotic and abiotic factors on R_s. Since the sample size was
311 relatively small (n = 88), the number of predictors included in the model was thoroughly
312 limited, as recommended by Shipley (2002). Our models considered a complete set of
313 hypothesis based on literature, previous exploratory analyses (Kruskal-Wallis, correlations,
314 etc.), and our own previous experience (Flores-Rentería et al., 2016, 2018; Pérez-Izquierdo
315 et al., 2017, see Fig. S2). The model assumed that aboveground vegetation structure (size of
316 the sampled living and dead trees, tree competition index, and the % of understory and
317 grass cover) would affect the abiotic (microclimate, pH) and the biotic (root demography)
318 soil environment, as well as the nutritional status (PC1) and the organic matter content
319 (PC2) in soils under trees. Overall, both R_H and R_s, would be strongly controlled by
320 changes in all these environmental factors which are ultimately controlled by the
321 aboveground vegetation structure.
322
323 Several SEMs were run and the best-fitted ones were finally selected according to the
324 covariance proximity between observed and expected data (goodness-of-fit $\chi 2$). From the
325 general model we used multigroup SEM to test whether the studied factors were linked by
326 the same causal structure in each tree status (dead or living) and to identify the paths that
327 did not behave similarly in the two conditions (Shipley, 2002; García-Camacho et al.,
328 2010). For this analysis, we used the same hypothetical model used for each status group
329 separately. A constrained model in which all free parameters were forced to be equal across
330 the two conditions was built and contrasted with field data. Since a lack of fit was detected
331 in the fully constrained multigroup model, a series of nested models, where equality
332 constraints were removed one at a time, were developed to detect which one would

significantly improve the model (Shipley, 2002; García-Camacho et al., 2010). Differences in X^2 and AIC statistics between the fully constrained model and the models freed from a constraint were used to test for differences in parameter values between the two conditions. Standardized path coefficients were estimated by using the maximum likelihood algorithm (Shipley, 2002). SEM analyses were performed using SPSS® and SPSS® AMOS 20.0 software's (IBM Corporation Software Group, Somers, NY).

3. Results

Both SWC and Tsoil varied significantly between years, being "year 1" (2016) warmer and wetter on average than "year 2" (2017), although no such significant trend was found for R_s (Figs. 1 and S3). No differences in R_s were found between the three conifer species, although the soils from Silver fir stands were significantly colder (lower average Tsoil) and wetter (higher average SWC) than the ones from the Black pine and Scots pine stands (Fig. S3). When looking for differences in SWC, Tsoil and R_s considering tree status (living or dead), living trees differed significantly from the dead ones only in SWC and R_s. Specifically, dead trees showed higher SWC and R_s values than the living ones (Figs. 1 and S3).

Overall, R_s was consistently higher under dead trees with respect to living ones (Fig. 2, Table S1). According to our results, CO_2 emissions under dead trees were on average 21% higher than under living ones. Furthermore, R_H, specific root length/area (SRL/SRA), TOC, TON, and SWC were among the environmental variables that were consistently higher, although not always significantly, under dead trees comparing with the living ones (Fig. 2, Table S1). Other variables such as pH, C:N ratio, or total fine root biomass/volume (FRB

and FRV, respectively) showed less sensitivity to tree mortality and/or less consistent trends across tree species, although FRB tended to be lower under dead trees (Fig. 2, Table S1). No clear differences were found between living and dead trees when the grass and understory cover, or the tree competition index were considered (Table S1). This happened because cover of understory of broadleaf seedlings and grasses was independent of the health status of the sampled trees and very dependent on site-specifics conditions.

Both mean soil temperature and quantity of SOM (PC2) were, together with tree status (living and death) the variables that better explained R_s variability across sites (Fig. 3, Table S1). As expected for ecosystems generally limited by temperature, Tsoil explained a large portion of across-site variability in R_s (Fig. 3, Table S2), whereas R_s was also strongly driven by SOM quantity (PC2, Fig. 3, Table S2). No differences in R_H between soil collected under dead and living trees were found (Figure 4). On the other hand, we found a strong effect of the nutritional status (PC1) and the quantity of SOM (PC2) on R_H (Fig. 4, Table S3). Additionally, the best obtained model also included a significant negative effect of SRL over R_H (Fig. 4, Table S3).

SEMs showed the complex causal-effect cascade of processes controlling R_s and R_H (Fig. 5). Specifically, this analyses highlighted how strongly forest structure (tree DBH, tree competition, understory and grass cover) influenced, directly or indirectly, the observed variability of soil abiotic (microclimate, pH, nutrient content) and biotic (SRL, FRV, R_H) variables, resulting in the observed variability in R_s across sites. Both, trees (i.e. size and tree competition) and understory cover exerted a strong effect over soil microclimate (Tsoil), soil pH, and nutrients (PC1). While conifers tend to acidify soils, we here observe

how an increasing cover of broadleaf understory was associated with increases in pH, which, on the other hand, was also behind the observed improvement of soil nutritional status (PC1) and SOM sequestration (PC2). The presence of grasses was also directly associated with an increase in SOM (PC2) and SRA, but a decrease in FRV. Multigroup SEM further showed a tighter control of Tsoil over R_s under dead than under living trees, as illustrated by the significantly higher ML coefficient obtained. Moreover, multigroup SEM also showed how conifers and successional vegetation exerted an opposite effect over the demography of fine roots (SRL and FRV). Specifically, living trees exerted an overall negative effect over SRL, whereas the presence of grasses was positively associated with SRL. On the other hand, the FRV was stimulated in poor soils (high PC1) and under high SOM contents (low PC2), but was also negatively correlated with the presence of grasses and the increase in broadleaf understory cover. Furthermore, we here show how, independently of the health status of the trees, increase in the SRA negatively affected R_H. Also, controls of R_H differed depending on the conifer health status (living or dead): living trees exerted a positive control over R_H, but when tree dies R_H variability was mainly controlled by nutrient status (PC1) and SOM quantity (PC2) (besides SRL). Finally, observed variability of R_s seemed to be partially explained by variability of R_H under dead trees while under living conifers no relation was found between both fluxes.

4. Discussion

We here reported large events of drought-induced tree mortality on stands dominated by three of the conifer tree species most widely distributed in the Carpathian mountain range (Table 1). This drought-induced mortality coincides with globally increasing reported events of conifer decline, which are being generally attributed to historical management

405 practices (e.g. favoring/planting conifer species outside their climatic and structural
406 optimum; Urbieta et al., 2008; Ruiz-Benito et al., 2012), or to climate-change induced
407 increases in temperature and droughts intensity and frequency that seem to affect more the
408 conifer-like than the angiosperms-like related functional traits (Henne Paul et al., 2015;
409 McIntyre et al., 2015; Ruiz-Benito et al., 2017). Indeed, the observed increasing presence of
410 an understory vegetation of seedlings mainly composed by native broadleaf species (e.g.
411 *Fagus sylvatica*, *Fraxinus excelsior*, *Fraxinus ornus*, *Acer campestre, Quercus petraea*,
412 *Ulmus glabra*) (Table 1) coincides with these mentioned above observations and are,
413 therefore, in accordance with this general decline in conifer dominance, especially
414 ubiquitously observed in European forests.
415
416 Drought induced conifer mortality resulted in large increases in biogenic soil CO_2
417 emissions (R_s), averaging a 21% increase under the dead trees comparing with the living
418 ones, and persisting during two consecutive years (2016-2017), four to five years after the
419 mortality event occurred in 2012. Given the observed large proportion of tree mortality
420 observed after the 2012 drought (Table 1), this tree mortality-induced hot-spot of CO_2
421 emissions might be responsible for decelerating the capacity of these ecosystems to recover
422 pre-mortality levels of C sequestration (e.g. Moore et al, 2013). Our results are not in
423 accordance with decreases in R_s observed under experimental tree girdling manipulations
424 (e.g. Högberg et al., 2001; Binkley et al., 2006; Nave et al., 2011; Levy-Varon et al., 2014),
425 or under natural conditions, when tree mortality events were massively caused by bark
426 beetle attacks (e.g. Moore et al. 2013) or by infections with pathogens, e.g. *Phytophtora*
427 *cinammoni* (Avila et al., 2016). Accordingly, literature generally shows how tree death

results in an almost immediate and dramatic decrease in R_s rates associated with the decrease in the supply of newly plants-fixed carbohydrate for belowground metabolic activity, e.g. autotrophic respiration, mycorrhiza activity and rhizosphere heterotrophic respiration (Subke et al., 2004; Högberg et al., 2007). This R_s drop associated with tree mortality may last for decades in monospecific forest (e.g. Moore et al. 2013, Avila et al., 2016), while other studies have shown how depending on the level of the perturbation and the secondary successional processes, R_s may recover pre-perturbation values after several years (e.g. Levy-Varon et al., 2014; Barba et al., 2016), or even increase during favorable seasons in mixed forest (Barba et al., 2013). Hence, due to the initial physiological collapse that tree mortality produces in a system, the functional recovery of this system in general and of the R_s in particular depends on the degree of perturbation but also on secondary successional process triggered by tree mortality (Levy-Varon et al., 2014; Lloret et al., 2015; Barba et al., 2018).

In these conifer forests so representative for the Carpathians' landscape, the observed hot-spots of CO_2 under dead trees were strongly dominated by R_H (Fig. 2 and 5). We here postulate that these mortality-triggered hot-spots of R_H and R_s were mostly explained by an increase in the quality and quantity of SOM which results from both the increase in senescent material and from the successional processes following tree death (Fig. 2, 4 and 5). The observed increase in topsoil SOM under dead trees (increase in TOC, Figure 2) could be attributed, at least partially, to the accumulation of senescent plant material (leaves, roots and branches) which generally accumulate under dead trees (Moore et al. 2013). However, SOM accumulation under dead conifers alone cannot explain the observed increase in R_H because, as observed, R_H was also very sensitive to the increase in soil

452 nutrient availability (PC1) (Figure 4, Table S3). Besides, we here observed how shifts in
453 the controls of R_s after the massive mortality event of 2012 ultimately resulted in a stronger
454 dominant role of the successional vegetation (broadleaf seedlings, shrubland and grasses)
455 over the belowground environmental factors, directly or indirectly affecting R_s and R_H
456 fluxes (Figure 5). This shift towards greater understory control over soil functions was in
457 detriment of the former control exerted by the conifers which influenced the microclimate
458 (SWC and Tsoil), the abiotic soil environment (pH), the nutrient quality (PC1), SOM
459 (PC2), and the fine root demography (specifically SRA/SRL, FRV) (Figs. 2, 3, 4 and 5).
460 These changes were further reflected in changes in the magnitude and the controls of biotic
461 soil fluxes (R_s and R_H) (Figure 2 and 5).
462
463 For instance, the increase in pH and grassland cover resulting from the shift in the
464 aboveground vegetation dominance also played a critical role in increasing SOM (PC2; Fig.
465 5). This is because, under conifer influence, the generally low soil pH and the low quality
466 of the residues due to the high proportion of recalcitrant compounds, e.g. lignin and/or
467 allelopathic molecules (e.g. Curiel Yuste et al. 2005; Fernández-Alonso et al., 2018) slow
468 down the breakdown of the litter and its incorporation to SOM in the mineral soil. On the
469 other hand, incorporation of litter in SOM occurs generally faster in ecosystems dominated
470 by broadleaf species because the generally higher pH and higher quality of the produced
471 residues stimulates bioturbation (Frouz et al., 2009). Indeed, the multigroup SEM further
472 showed how the increase in pH associated with the increasing presence of the understory
473 vegetation had a direct and strong positive effect over SOM quality (PC1), suggesting that
474 on top of the increase in SOM under dead trees, the secondary successional processes
475 triggered by conifer mortality was positively affecting the quality of the substrate. Our

476 results, therefore, clearly indicate how the shift in vegetation dominance associated with
477 conifer mortality had a strong impact over the quantity and quality of SOM, resulting in
478 increased R_H, which subsequently affected R_s.
479
480 This dominant role of successional vegetation after tree death was also reflected in a
481 substantial increase in the surface of absorption of the radical system (increase in SRL and
482 SRA; Fig. 2) which corresponds to a shift towards a fine-root demography optimized to
483 maximize nutrients acquisition (Roumet et al., 2016). This shift, associated with an increase
484 in the presence of grasses (Fig. 5), suggest that the belowground niche left by the death of
485 the conifers creates an opportunity to the surrounding early successional vegetation to
486 obtain resources (nutrients and moisture) (Curiel Yuste et al., 2012; Barba et al., 2013)
487 whose acquisition is, otherwise, subjected to strong competition, especially in nutrient-
488 poor, low pH conifer sites as those considered in this study. Indeed, the multigroup SEM
489 showed how the poor nutrient conditions under conifers (PC1), while alive, promoted a
490 bigger radical system (higher FRV), but with relatively less very fine roots (suppressing
491 SRL).
492
493 The consistent increase in the specific length and surface (SRL/SRA) of fine roots under
494 dead trees was paralleled by the observed increase in R_s (Figure 2). This was expected,
495 given the general observed linear relation between, on one hand, SRL and the fine roots
496 turnover rates (Silver and Miya, 2001; Hobbie et al., 2010; Roumet et al., 2016), and, on
497 the other hand, SRL and rates of root respiration (R_A) (Reich et al., 2008; Makita et al.,
498 2012; Picon-Cochard et al., 2012). Although R_A were not measured in this study, we did
499 not observe a significant increase in SOM turnover (rates of R_H per unit of soil C; data not

shown) under dead trees, suggesting that it is most plausible that the increase of SRL was associated with a parallel increase in R_A. Rather than stimulating R_H, our models also showed a very consistent negative relation between SRL and R_H (Figure 4 and 5), suggesting that besides this expected positive effect of SRL over autotrophic activity, the net effect over R_H was negative. It, therefore, could be that by increasing their capacity to absorb nutrients (increase in SRL), successional vegetation competes more efficiently for the same resources with the soil heterotrophic community (negative priming, Kuzyakov 2002), resulting in the observed suppression of R_H. Indeed, an increase in competition for key nutrients (e.g. N, P, K) between roots and heterotrophs could be maximal in soils when nutrients are generally limiting, thereby resulting in the suppression of R_H (e.g. Schimel et al., 1989; Wang and Bakken 1997; Kuzyakov 2002).

5. Conclusions

We here collected compelling evidences to support our initial hypotheses: cascading mechanisms triggered by selective tree mortality and a subsequent secondary successional process played a critical role in regulating soil functioning and soil CO_2 emissions during transitional states. Specifically, we here show how conifer mortality resulted in an average increment of biogenic emissions of 21%, 4-5 years after the large mortality event of 2012, which might be further responsible for decelerating the capacity of these ecosystems to recover pre-mortality levels of C sequestration. These transitional states after tree death resulted in a stimulation of the heterotrophic activity (R_H), favored by the increase in senescent material but also by changes in the soil microenvironment (e.g. climate, pH and SOM) partially controlled by successional vegetation. A shift towards a more efficient resource-acquisitive strategy of fine roots (increase in SRL), triggered by tree mortality and

524 also associated with the increasing dominance of the successional vegetation, was also
525 behind the observed changes in the magnitude and controls of R_H and R_s. Our results,
526 hence, call the attention on how above-belowground ecological processes triggered by tree
527 mortality may substantially determine dynamics of key biogeochemical cycles (e.g. C and
528 N) at local and regional scales. One of the drawbacks of this study might be the fact that the
529 effects of tree-mortality were only evaluated during a relatively short-term (2 years), at sub-
530 decadal time scale (4-5 years after the main mortality event), and in a limited number of
531 sites (9). Despite its limitations, this is one of the first studies evidencing the complexity of
532 the controls over R_s in climate-change-induced tree mortality scenarios, and as such, it
533 might serve as a base to develop further, more extended studies on this topic. In a changing
534 world where episodes of tree mortality associated with climate change are substantially
535 incrementing, more studies should, therefore, be designed to deepen the observed potential
536 impacts of tree mortality and subsequent successional processes at larger temporal and
537 spatial scales
538
539 **Acknowledgements**
540 The authors thanks to the staff of Forest Districts: Kronstadt, Rasnov, Codlea, Teliu, and
541 Sacele who administrate the 9 forests considered for this study. This work was supported
542 by the Spanish Ministry of Economy and Competitiveness (MINECO) with the projects
543 VERONICA (CGL2013-42271-P) and the project IBERYCA (CGL2017-84723-P), and by
544 the Romanian Ministry of Education and Scientific Research through UEFISCDI with the
545 projects TREEMORIS (PN-II-RU-TE-2014-4-0791), NATIvE (PN-III-P1-1.1-PD-2016-
546 0583), and BIOCARB (PN-III-P1-1.1-TE-2016-1508). This research was also supported by
547 the Basque Government through the BERC 2018-2021 program, and by the Spanish

Ministry of Economy and Competitiveness (MINECO) through the BC3 María de Maeztu excellence accreditation (MDM-2017-0714). I.C. Petritan was partially funded by the H2020/ERA-NET/ERA-GAS (Project 82/2017, Mobilizing and monitoring climate positive efforts in forests and forestry, FORCLIMIT). Many thanks to Cosmin Zgremtia, Ionela Medrea, Andrei Apafaian, Raluca Enescu and Marta Ramos for their valuable help during field campaigns and laboratory work.

556 **Bibliography**

557 Allen, C.D., Macalady, A.K., Chenchouni, H., Bachelet, D., McDowell, N., Vennetier, M.,
558 Kitzberger, T., Rigling, A., Breshears, D.D., Hogg, E.H., Gonzalez, P., Fensham, R.,
559 Zhang, Z., Castro, J., Demidova, N., Lim, J.-H., Allard, G., Running, S.W., Semerci, A.,
560 Cobb, N., 2010. A global overview of drought and heat-induced tree mortality reveals
561 emerging climate change risks for forests. Forest Ecology and Management 259, 660-684.
562 Allen Craig, D., Breshears David, D., McDowell Nate, G., 2015. On underestimation of
563 global vulnerability to tree mortality and forest die-off from hotter drought in the
564 Anthropocene. Ecosphere 6, art129.
565 Anderegg, W.R.L., Berry, J.A., Field, C.B., 2012. Linking definitions, mechanisms, and
566 modeling of drought-induced tree death. Trends in Plant Science 17, 693-700.
567 Avila, J.M., Gallardo, A., Ibáñez, B., Gómez-Aparicio, L., 2016. Quercus suber dieback
568 alters soil respiration and nutrient availability in Mediterranean forests. Journal of Ecology
569 104, 1441-1452.
570 Avila, J.M., Gallardo, A., Gómez- Aparicio, L., 2018. Pathogen-induced tree mortality
571 interacts with predicted climate change to alter soil respiration and nutrient availability in
572 Mediterranean systems. Biogeochemistry, 142, (1), 53–71
573 Barba, J., Curiel Yuste, J., Martínez-Vilalta, J., Lloret, F., 2013. Drought-induced tree
574 species replacement is reflected in the spatial variability of soil respiration in a mixed
575 Mediterranean forest. Forest Ecology and Management 306, 79-87.
576 Barba, J., Curiel Yuste, J., Poyatos, R., Janssens, I.A., Lloret, F., 2016. Strong resilience of
577 soil respiration components to drought-induced die-off resulting in forest secondary
578 succession. Oecologia, 1-15.

579 Barba, J., Lloret, F., Poyatos, R., Molowny-Horas, R., Yuste, J., 2018. Multi-temporal
580 influence of vegetation on soil respiration in a drought-affected forest. iForest -
581 Biogeosciences and Forestry 11, 189-198.
582 Binkley, D., Stape, J.L., Takahashi, E.N., Ryan, M.G., 2006. Tree-girdling to separate root
583 and heterotrophic respiration in two Eucalyptus stands in Brazil. Oecologia 148, 447-454.
584 Birch, H.F., 1958. The effect of soil drying on humus decomposition and nitrogen
585 availability. Plant and Soil 10, 9-31.
586 Carnicer, J., Coll, M., Ninyerola, M., Pons, X., Sánchez, G., Peñuelas, J., 2011. Widespread
587 crown condition decline, food web disruption, and amplified tree mortality with increased
588 climate change-type drought. Proceedings of the National Academy of Sciences 108, 1474.
589 Curiel Yuste, J., Barba, J., Fernandez-Gonzalez, A.J., Fernandez-Lopez, M., Mattana, S.,
590 Martinez-Vilalta, J., Nolis, P., Lloret, F., 2012. Changes in soil bacterial community
591 triggered by drought-induced gap succession preceded changes in soil C stocks and quality.
592 Ecology and Evolution 2, 3016-3031.
593 Curiel Yuste, J., Janssens, I.A., Carrara, A., Meiresonne, L., Ceulemans, R., 2003.
594 Interactive effects of temperature and precipitation on soil respiration in a temperate
595 maritime pine forest. Tree Physiology 23, 1263-1270.
596 Curiel Yuste, J., Nagy, M., Janssens, I.A., Carrara, A., Ceulemans, R., 2005. Soil
597 respiration in a mixed temperate forest and its contribution to total ecosystem respiration.
598 Tree Physiology 25, 609-619.
599 Davidson Eric, A., Janssens Ivan, A., Luo, Y., 2005. On the variability of respiration in
600 terrestrial ecosystems: moving beyond Q10. Global Change Biology 12, 154-164.
601 Eissenstat, D.M., Wells, C.E., Yanai, R.D., Whitbeck, J.L., 2000. Building roots in a
602 changing environment: implications for root longevity. New Phytologist 147, 33-42.

603 Fernández-Alonso, M.J., Curiel Yuste, J., Kitzler, B., Ortiz, C., Rubio, A., 2018. Changes
604 in litter chemistry associated with global change-driven forest succession resulted in time-
605 decoupled responses of soil carbon and nitrogen cycles. Soil Biology and Biochemistry
606 120, 200-211.
607 Flores-Rentería, D., Curiel Yuste, J., Rincón, A., Brearley, F., García-Gil, J., Valladares, F.,
608 2015. Habitat fragmentation can modulate drought effects on the plant-soil-microbial
609 system in Mediterranean holm oak (*Quercus ilex*) forests. Microbial Ecology 69, 798-812.
610 Flores-Rentería, D., Curiel Yuste, J., Valladares, F., Rincón, A., 2018. Soil legacies
611 determine the resistance of an experimental plant-soil system to drought. CATENA 166,
612 271-278.
613 Flores-Rentería, D., Rincón, A., Valladares, F., Curiel Yuste, J., 2016. Agricultural matrix
614 affects differently the alpha and beta structural and functional diversity of soil microbial
615 communities in a fragmented Mediterranean holm oak forest. Soil Biology and
616 Biochemistry 92, 79-90.
617 Frouz, J., Pižl, V., Cienciala, E., Kalčík, J., 2009. Carbon storage in post-mining forest soil,
618 the role of tree biomass and soil bioturbation. Biogeochemistry 94, 111-121.
619 García-Camacho, R., Iriondo, J.M., Escudero, A., 2010. Seedling dynamics at elevation
620 limits: Complex interactions beyond seed and microsite limitations. American Journal of
621 Botany 97, 1791-1797.
622 Gazol, A., Camarero, J.J., Jiménez, J.J., Moret-Fernández, D., López, M.V., Sangüesa-
623 Barreda, G., Igual, J.M., 2018. Beneath the canopy: Linking drought-induced forest die off
624 and changes in soil properties. Forest Ecology and Management 422, 294-302.
625 Gough Christopher, M., Hardiman Brady, S., Nave Lucas, E., Bohrer, G., Maurer Kyle, D.,
626 Vogel Christoph, S., Nadelhoffer Knute, J., Curtis Peter, S., 2013. Sustained carbon uptake

627 and storage following moderate disturbance in a Great Lakes forest. Ecological
628 Applications 23, 1202-1215.
629 Henne Paul, D., Elkin, C., Franke, J., Colombaroli, D., Calò, C., La Mantia, T., Pasta, S.,
630 Conedera, M., Dermody, O., Tinner, W., 2015. Reviving extinct Mediterranean forest
631 communities may improve ecosystem potential in a warmer future. Frontiers in Ecology
632 and the Environment 13, 356-362.
633 Hobbie, S.E., Oleksyn, J., Eissenstat, D.M., Reich, P.B., 2010. Fine root decomposition
634 rates do not mirror those of leaf litter among temperate tree species. Oecologia 162, 505-
635 513.
636 Högberg, M.N., Högberg, P., Myrold, D.D., 2007. Is microbial community composition in
637 boreal forest soils determined by pH, C-to-N ratio, the trees, or all three? Oecologia 150,
638 590-601.
639 Högberg, P., Nordgren, A., Buchmann, N., Taylor, A.F.S., Ekblad, A., Högberg, M.N.,
640 Nyberg, G., Ottosson-Löfvenius, M., Read, D.J., 2001. Large-scale forest girdling shows
641 that current photosynthesis drives soil respiration. Nature 411, 789.
642 Janssens, I.A., Lankreijer, H., Matteucci, G., Kowalski, A.S., Buchmann, N., Epron, D.,
643 Pilegaard, K., Kutsch, W., Longdoz, B., Grünwald, T., Montagnani, L., Dore, S., Rebmann,
644 C., Moors, E.J., Grelle, A., Rannik, Ü., Morgenstern, K., Oltchev, S., Clement, R.,
645 Guðmundsson, J., Minerbi, S., Berbigier, P., Ibrom, A., Moncrieff, J., Aubinet, M.,
646 Bernhofer, C., Jensen, N.O., Vesala, T., Granier, A., Schulze, E.D., Lindroth, A., Dolman,
647 A.J., Jarvis, P.G., Ceulemans, R., Valentini, R., 2002. Productivity overshadows
648 temperature in determining soil and ecosystem respiration across European forests. Global
649 Change Biology 7, 269-278.

650 Levy-Varon, J.H., Schuster, W.S.F., Griffin, K.L., 2014. Rapid rebound of soil respiration
651 following partial stand disturbance by tree girdling in a temperate deciduous forest.
652 Oecologia 174, 1415-1424.
653 Lloret, F., Kitzberger, T., 2018. Historical and event-based bioclimatic suitability predicts
654 regional forest vulnerability to compound effects of severe drought and bark beetle
655 infestation. Global Change Biology 24, 1952-1964.
656 Lloret, F., Mattana, S., Curiel Yuste, J., 2015. Climate-induced die-off affects plant–soil–
657 microbe ecological relationship and functioning. FEMS Microbiology Ecology 91, 1-12.
658 Makita, N., Kosugi, Y., Dannoura, M., Takanashi, S., Niiyama, K., Kassim, A.R., Nik,
659 A.R., 2012. Patterns of root respiration rates and morphological traits in 13 tree species in a
660 tropical forest. Tree Physiology 32, 303-312.
661 McDowell, N.G., Williams, A.P., Xu, C., Pockman, W.T., Dickman, L.T., Sevanto, S.,
662 Pangle, R., Limousin, J., Plaut, J., Mackay, D.S., Ogee, J., Domec, J.C., Allen, C.D.,
663 Fisher, R.A., Jiang, X., Muss, J.D., Breshears, D.D., Rauscher, S.A., Koven, C., 2015.
664 Multi-scale predictions of massive conifer mortality due to chronic temperature rise. Nature
665 Climate Change 6, 295.
666 McIntyre, P.J., Thorne, J.H., Dolanc, C.R., Flint, A.L., Flint, L.E., Kelly, M., Ackerly,
667 D.D., 2015. Twentieth-century shifts in forest structure in California: Denser forests,
668 smaller trees, and increased dominance of oaks. Proceedings of the National Academy of
669 Sciences 112, 1458.
670 Nave, L.E., Gough, C.M., Maurer, K.D., Bohrer, G., Hardiman, B.S., Le Moine, J., Munoz,
671 A.B., Nadelhoffer, K.J., Sparks, J.P., Strahm, B.D., Vogel, C.S., Curtis, P.S., 2011.
672 Disturbance and the resilience of coupled carbon and nitrogen cycling in a north temperate
673 forest. Journal of Geophysical Research: Biogeosciences 116.

674 Neumann, M., Mues, V., Moreno, A., Hasenauer, H., Seidl, R., 2017. Climate variability
675 drives recent tree mortality in Europe. Global Change Biology 23, 4788-4797.
676 Pérez-Izquierdo, L., Zabal-Aguirre, M., Flores-Rentería, D., González-Martínez, S.C.,
677 Buée, M., Rincón, A., 2017. Functional outcomes of fungal community shifts driven by
678 tree genotype and spatial-temporal factors in Mediterranean pine forests. Environmental
679 Microbiology 19, 1639-1652.
680 Picon-Cochard, C., Pilon, R., Tarroux, E., Pagès, L., Robertson, J., Dawson, L., 2012.
681 Effect of species, root branching order and season on the root traits of 13 perennial grass
682 species. Plant and Soil 353, 47-57.
683 Reich Peter, B., Tjoelker Mark, G., Pregitzer Kurt, S., Wright Ian, J., Oleksyn, J., Machado,
684 J.L., 2008. Scaling of respiration to nitrogen in leaves, stems and roots of higher land
685 plants. Ecology Letters 11, 793-801.
686 Rogers Brendan, M., Jantz, P., Goetz Scott, J., 2016. Vulnerability of eastern US tree
687 species to climate change. Global Change Biology 23, 3302-3320.
688 Roumet, C., Birouste, M., Picon-Cochard, C., Ghestem, M., Osman, N., Vrignon-Brenas,
689 S., Cao, K.f., Stokes, A., 2016. Root structure–function relationships in 74 species:
690 evidence of a root economics spectrum related to carbon economy. New Phytologist 210,
691 815-826.
692 Ruiz-Benito, P., Gómez-Aparicio, L., Zavala, M.A., 2012. Large-scale assessment of
693 regeneration and diversity in Mediterranean planted pine forests along ecological gradients.
694 Diversity and Distributions 18, 1092-1106.
695 Ruiz-Benito, P., Ratcliffe, S., Zavala, M.A., Martínez-Vilalta, J., Vilà-Cabrera, A., Lloret,
696 F., Madrigal-González, J., Wirth, C., Greenwood, S., Kändler, G., Lehtonen, A., Kattge, J.,

697 Dahlgren, J., Jump, A.S., 2017. Climate- and successional-related changes in functional
698 composition of European forests are strongly driven by tree mortality. Global Change
699 Biology 23, 4162-4176.
700 Sangüesa-Barreda, G., Linares, J.C., Camarero, J.J., 2015. Reduced growth sensitivity to
701 climate in bark-beetle infested Aleppo pines: Connecting climatic and biotic drivers of
702 forest dieback. Forest Ecology and Management 357, 126-137.
703 Shipley, B., 2002. Cause and correlation in biology: a user's guide to path analysis,
704 structural equations and causal inference. Cambridge University Press, Cambridge, UK.
705 Silver, W.L., Miya, R.K., 2001. Global patterns in root decomposition: comparisons of
706 climate and litter quality effects. Oecologia 129, 407-419.
707 Subke, J.-A., Hahn, V., Battipaglia, G., Linder, S., Buchmann, N., Cotrufo, M.F., 2004.
708 Feedback interactions between needle litter decomposition and rhizosphere activity.
709 Oecologia 139, 551-559.
710 Tang, J., Baldocchi Dennis, D., Xu, L., 2005. Tree photosynthesis modulates soil
711 respiration on a diurnal time scale. Global Change Biology 11, 1298-1304.
712 Urbieta, I.R., Zavala, M.A., Marañón, T., 2008. Human and non-human determinants of
713 forest composition in southern Spain: evidence of shifts towards cork oak dominance as a
714 result of management over the past century. Journal of Biogeography 35, 1688-1700.
715 van der Heijden, M.G.A., Bardgett, R.D., Van Straalen, N.M., 2008. The unseen majority:
716 soil microbes as drivers of plant diversity and productivity in terrestrial ecosystems.
717 Ecology Letters 11, 296-310.

718 Vargas, R., Detto, M., Baldocchi Dennis, D., Allen Michael, F., 2010. Multiscale analysis
719 of temporal variability of soil CO2 production as influenced by weather and vegetation.
720 Global Change Biology 16, 1589-1605.
721 Vayreda, J., Martínez-Vilalta, J., Vilà-Cabrera, A., 2016. El Inventario Ecológico y Forestal
722 de Cataluña: una herramienta para la ecología funcional. Revista Ecosistemas 25, 70-79.
723

Fig. captions

Fig. 1. Evolution of soil water content (SWC), soil temperature (Tsoil) and soil respiration (R_s) as a function of time and trees' health status (living or dead). Error bars represent the standard error of the mean.

Fig. 2. Changes in soil abiotic (microclimate, pH) and biotic (fine root demography, R_s, R_H) variables, as well as soil total organic carbon (TOC) and total organic nitrogen (TON) values evaluated under dead trees relative to the values evaluated under living trees. Therefore, positive values (right hand side of the vertical bar) represent an increase in that particular variable under dead with respect to under living trees. Error bars represent standard error of the mean. Asterisk represent significant from zero differences (p value > 0.05; t-test).

Fig. 3. Linear mixed-effects models for soil respiration (R_s). Solid lines represent modeled R_s responses under dead trees, whereas dotted lines represent modeled R_s responses under living trees. Where, Ts = soil temperature at 5 cm depth; PC2 = second dimension of the PCA, here representing SOM.

Fig. 4. Linear mixed-effects models for heterotrophic respiration (R_H). Solid lines represent modeled R_s responses under dead trees, whereas dotted lines represent modeled R_s responses under living trees. SRL = specific root length; PC1= first dimension of the PCA, here representing soil nutrients; PC2 = second dimension of the PCA, here representing SOM.

Fig. 5. Multigroup SEM representation. Path diagrams representing hypothesized causal relationships between aboveground vegetation, biotic and abiotic variables, soil respiration (R_s) and soil heterotrophic activity (R_H) under living (a) and dead (b) conifer trees. Arrows depict causal relationships: positive and negative effects are indicated by solid and dashed lines respectively, with numbers indicating standardized estimated regression weights (SRW). Arrow widths are proportional to the significance values according to the legend. Paths with non-significant coefficients are represented in gray. Coefficients in bold characters represent those causal relationships where the strength of the relation differed between soils under living (green) and under dead (orange) trees. χ^2= 86.81, NFI= 0.83 y RMSEA= <0.0001, df= 122, p= 0.99

				Mort	Alt	SL	OR	MAP	MAT	DBH	Height	CAP	Age	LAI	UC	GC
site	species	Coordinates	Soil Type	%	m.a.s.l.	Deg	Deg	mm	ºC	cm	m	m^2	y	m^2/m^2	%	%
DAMBU MORII	AA	45°34'47.86"N	Eutricambisol	21	825	37	234	593	6.4	55	28	32	147	3.5	23 (7Fs3Aa)	18
KRONSTADT	AA	45°34'59.54"N	Eutricambisol	23	945	37	213	593	6.4	50	30	23	149	3.6	20 (9Fs1Aa)	53
RASNOV	AA	45°29'32.48"N	Eutricambisol litic	19	1250	37	213	693	3.7	54	30	30	145	3.6	8 (6Fs3Pa1Aa)	34
LEMPES	PN	45°43'31.50"N	Eutricambisol	27	561	17	225	593	6.4	39	23	27	99	3.4	41 (2Tc2Fs3Ap1Ug1Ac1Fo)	19
RACADAU	PN	45°37'58.37"N	Leptosol	16	753	30	121	593	6.4	43	24	28	96	4.3	69 (5Fo3Ug1Tc1Ac)	9
SCHEI	PN	45°37'56.32"N	Litic rendzina	18	456	36	117	593	6.4	45	25	30	97	3.8	55 (2Tc1Ac1Ug1Cb3Ap2Fs1Fo)	10
LEMPES	PS	45°44'6.75"N	Eutricambisol	22	545	24	115	593	6.4	37	19	20	111	2.7	68 (9Fe1Ug)	73
CODLEA	PS	45°42'9.70"N	Eutricambisol	18	712	18	139	599	6.6	45	24	21	115	3.3	37 (2Ap4Cb1Ug2Ac1Fs)	29
TELIU	PS	45°41'55.69"N	Regosol	17	606	33	190	601	5.6	40	25	28	114	3.9	7 (2Fs4Cb1Ac2Qp1Ps)	4

Table 1. Location, identity of the dominant conifer and structural characteristics of the 9 different sites under study. Mort= Mortality rate (%); Alt= Site Altitude (m); SL = Slope (º); OR= Orientation (º); MAP= mean annual precipitation (mm); MAT= mean annual temperature (ºC); DBH =diameter of breast height (cm), CAP= canopy area (m^2); LAI- leaf area index, UC= Understory cover(%), GC = Grassland cover (%); Understorey cover= (*Fs-Fagus sylvatica, Fo-Fraxinus ornis, Fe-Fraxinus excelsior, Pa-Picea abies, Cb-Carpinus betulus, Ug-Ulmus glabra, Ac-Acer campestre, Tc-Tilia cordata, Ap-Acer platanoides and Acer pseudoplatanus, Qp-Quercus petraea, Ps-Pinus sylvestris, Aa-Abies alba*)

Fig.1
Click here to download high resolution image

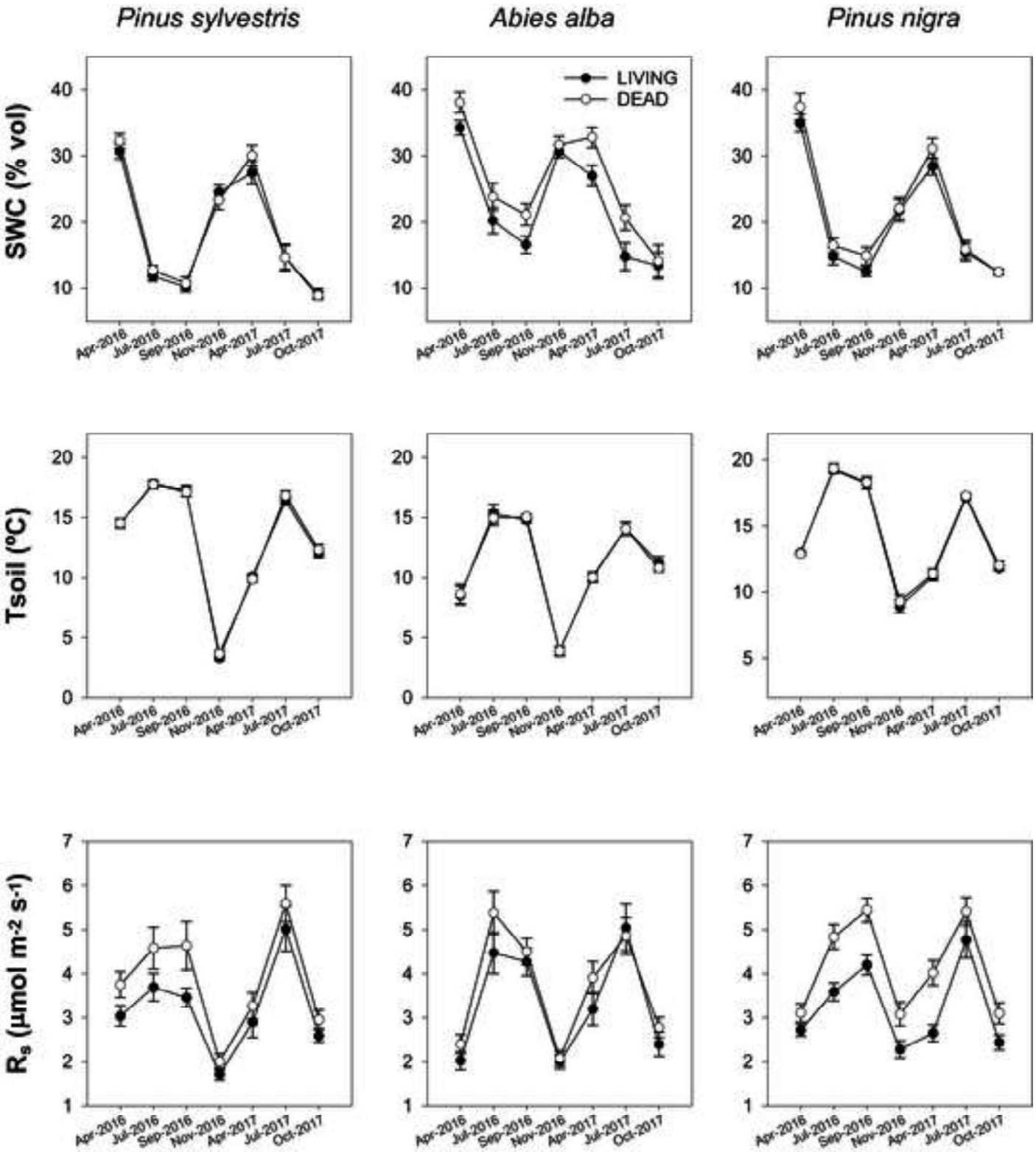

Fig.2

Click here to download high resolution image

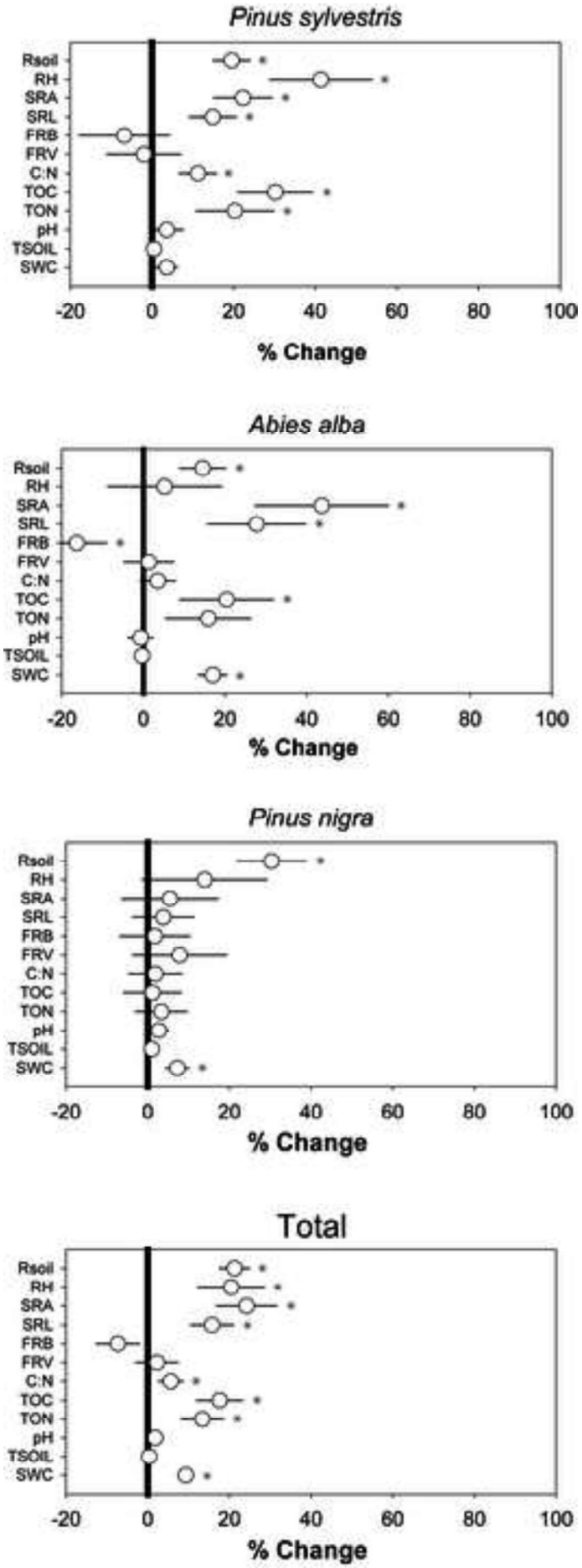

Fig.3
Click here to download high resolution image

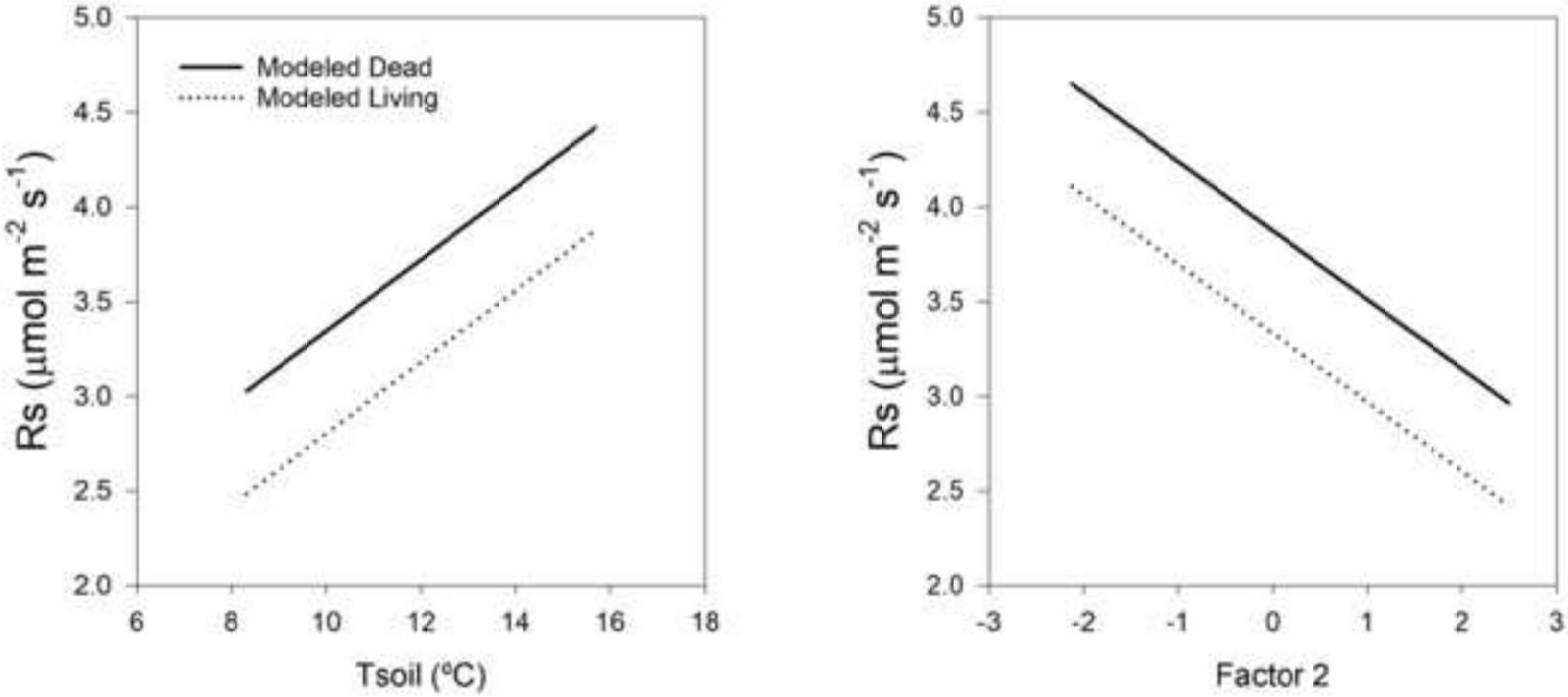

Fig.4

Click here to download high resolution image

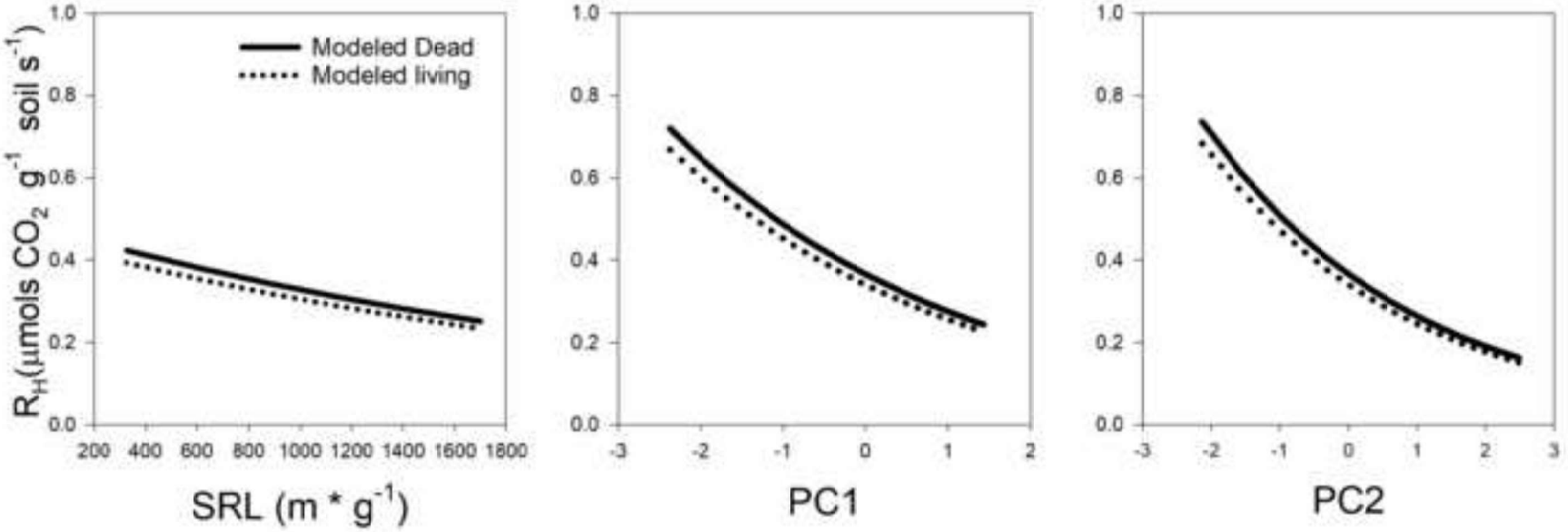

Fig.5

Click here to download high resolution image

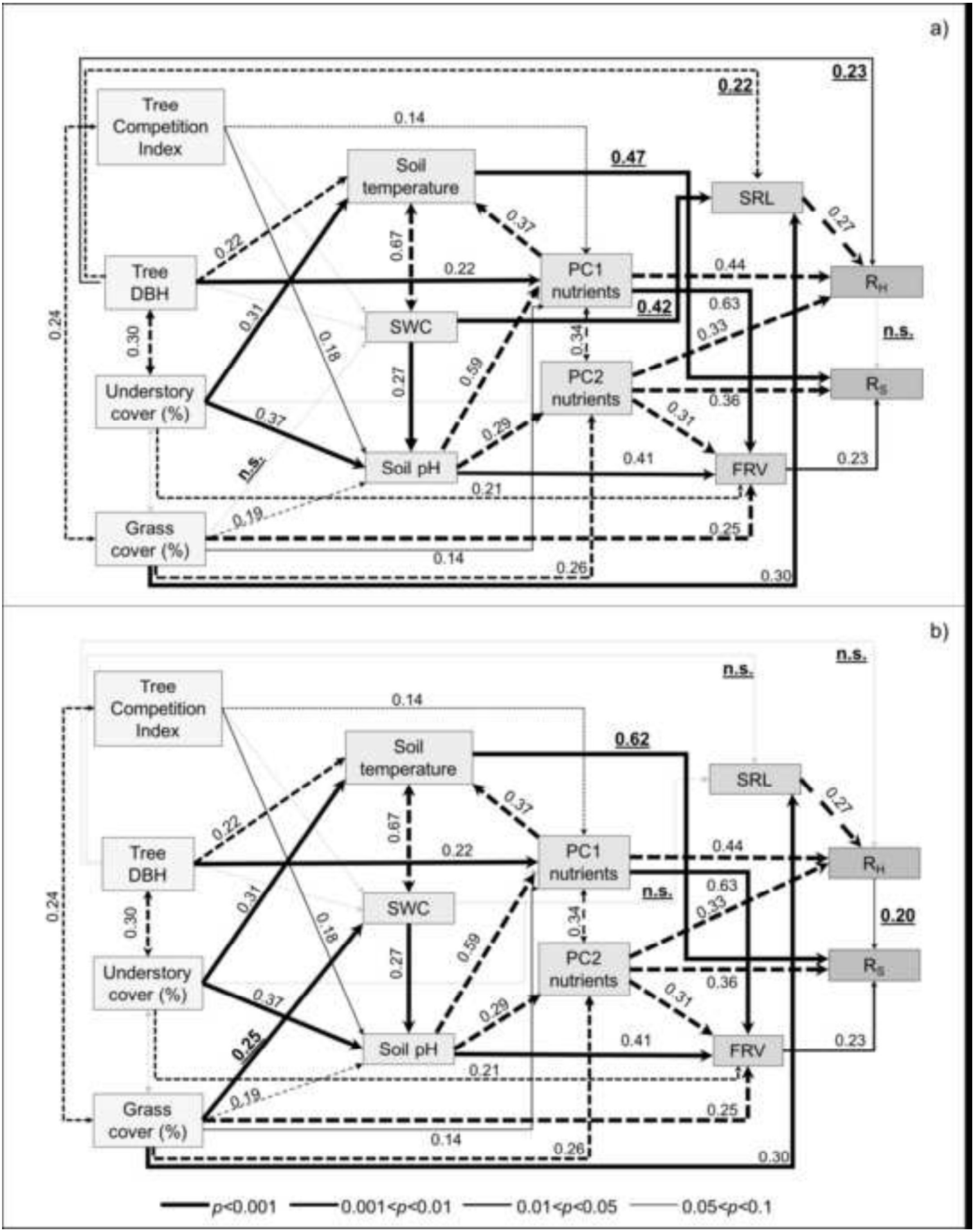

Supplementary Material for online publication only

Click here to download Supplementary Material for online publication only: NEW Suplementary materials SBB Curiel Yuste et al.